IgA dysfunction induced by the early-lifetime disruption of gut microbiota aggravates diet–induced metabolic syndrome in mice

Jielong Guo
China Agricultural University
Xue Han
China Agricultural University
Yilin You
China Agricultural University
Weidong Huang
China Agricultural University
Zhan Jicheng (zhanjicheng@cau.edu.cn)
China Agricultural University https://orcid.org/0000-0001-8757-7862

Research

Keywords: IgA, gut microbiota, metabolic syndrome, Low-dose penicillin, fecal microbiota transplantation, probiotics

Posted Date: April 20th, 2021

DOI: https://doi.org/10.21203/rs.3.rs-40336/v2

Abstract

Background

Low-dose antibiotic contamination in animal food is still a severe food safety problem worldwide. Penicillin is one of the main classes of antibiotics being detected in food. Previous studies have shown that transient exposure of low-dose penicillin (LDP) during early life resulted in metabolic syndrome (MetS) in mice. However, the underlying mechanism(s) and efficient approaches to counteracting this are largely unknown.

Methods

Wild-type (WT) or secretory IgA (SIgA)-deficient (*Pigr*$^{-/-}$) C57BL/6 mice were exposed to LDP or not from several days before birth to 30 d of age. Five times of FMT or probiotics (a mixture of *Lactobacillus bulgaricus* and *L. rhamnosus* GG) treatments were applied to parts of these LDP-treated mice from 12 d to 28 d of life. Bacterial composition from different regions (mucosa and lumen) of the colon and ileum were analyzed through 16S rDNA sequencing. Intestinal IgA response was analyzed. Multiple parameters related to MetS were also determined. In addition, germ-free animals and in vitro tissue culture were also used to determine the correlations between LDP, gut microbiota (GM) and intestinal IgA response.

Results

LDP disturbed the intestinal bacterial composition, especially for ileal mucosa, the main inductive and effective sites of IgA response, in 30-d-old mice. The alteration of early GM resulted in a persistent inhibition of the intestinal IgA response, leading to a constant reduction of fecal and caecal SIgA levels throughout the 25-week experiment, which is early life-dependent, as transfer of LDP-GM to 30 d germ-free mice only resulted in a transient reduction in fecal SIgA. LDP-induced reduction in SIgA led to a decrease in IgA+ bacteria and a dysbiosis in the ileal mucosal samples of 25 week wild-type but not *Pigr*$^{-/-}$ mice. Moreover, LDP also resulted in increases in ileal bacterial encroachment and adipose inflammation, along with an enhancement of diet-induced MetS in an intestinal SIgA-dependent manner. Furthermore, several times of FMT or probiotic treatments during LDP treatment are efficient to fully (for FMT) or partially (for probiotics) counteract the LDP-effect on both GM and metabolism.

Conclusions

Early-life LDP-induced enhancement of diet-induced MetS is mediated by intestinal SIgA, which could be (partially) restored by FMT or probiotics treatment.

Background

The early-lifetime period is critical for the development of immunity and metabolism, since the correct colonization and maturation of GM are delicately controlled by the host, and has a lifelong impact on the health of the host [1-5]. The disruption of the neonatal microbiome can result in lifelong changes in the GM

composition and has been linked to various conditions such as obesity, asthma, and inflammatory bowel disease (IBD) [6-9]. A main factor disturbing the establishment and maturation of the early GM is the exposure to antibiotics through therapeutic treatment (high dose) or unnoticed subtherapeutic exposure to low-dose antibiotics in contaminated animal foods (for example, meat, eggs, milk, and aquatic products) [1].

Overuse of antibiotics to young children for medical purpose in the US and China is pretty serious [1, 10] while efforts has been made in recent years by the government to reduce the therapeutic usage of antibiotics [11]. However, in contrast to therapeutic usage of antibiotics, low-dose antibiotics exposure via contaminated animal food is more inconspicuous and hard to avoid. In the USA, an estimated number of 17 million kg of antibiotics were used in farm animals as compared to an estimated 4 million kg in human per year and a majority number of these antibiotics is given in subtherapeutic doses to healthy chicken, cattle and pigs to promote weight gain [12]. A more severe overuse of animal antibiotics has also been reported in China, which results in considerable antibiotic residues in animal foods [13-15].

Penicillin is still one of the main antibiotics being used for animals and detected in contaminated food [1, 15]. Previous studies have shown that short-term low-dose penicillin (LDP) treatment during early life time transiently disturbed the fecal microbiota and resulted in metabolic syndrome (MetS) in mice [3, 16]. However, the underlying mechanisms, difference of microbial composition between intestinal luminal and mucosal samples, and efficient therapies of this LDP-induced dysbiosis and MetS were still largely unknown [3].

It has been previously reported that transient high-dose antibiotics treatment during early life resulted in a relatively long-lasted (up to 70 d of age) reduction in fecal SIgA [17-18], which is the most abundant immunoglobulin isotype in humans and mice and is a master controller of GM that has key role in regulating MetS [19]. However, the prolonged influence of high-dose antibiotics on the intestinal SIgA and its correlation with metabolic disease was not determined [17-18].

We then wondered whether IgA response plays a role in mediating the LDP-induced MetS. By using this LDP-induced MetS mouse model [3] as well as high-dose penicillin (HDP), we found that similar to high-dose antibiotics, transient LDP treatment dampens intestinal IgA response. However, surprisingly, with respect to the relatively short-time influence of transient HDP on fecal SIgA and intestinal IgA+ B cells (up to 8 weeks of age), LDP treatment persistently reduced fecal SIgA and intestinal IgA+ B cells (at least to 25 weeks of age, the end of the experiment). We also found that this persistent influence of LDP on IgA response was both GM- and early life-dependent. Moreover, using SIgA-deficient (*Pigr*$^{-/-}$) mice, we demonstrated that transient LDP treatment increased the ileal bacterial encroachment and translocation, leading to the exaggerated diet-induced MetS in WT mice in a SIgA-dependent manners. Lastly, we investigated the efficiency of FMT and probiotics in treating LDP-effect and found that several times of FMT and probiotic treatments during the LDP-treating period are enough to fully (for FMT) or partially (for probiotic) counteract the influences of LDP on MetS.

Results

LDP treatment affected the early microbiota

Study 1 design (Figure 1A): Nine-week-old wild-type (WT) female and male C57BL/6 mice were randomly paired (1:1) and co-housed for 4 d (one estrous cycle for house mouse). After co-housing, females was separated from males and fed solely and pregnancies and due dates were speculated according to the body weight changes. Several days before birth, pups were exposed to LDP (10 mg/L, ~1.5 mg/kg body weight)[3] through their mothers or drinking water until 30 d of age (LDP, F and P groups) or not (Ctr group). At 12d, 16d, 20d, 24d and 28d of age, the pups were gavaged with sterilized pre-reduced PBS (Ctr and LDP groups), and fecal microbiota (F group, pooled fecal samples from Ctr mice with a concentration ~ 0.3 g feces/mL PBS) or probiotics (P group, a bacterial mixture of *Lactobacillus bulgaricus* and *L. rhamnosus* GG (LGG) at ~10^8/mL for each bacterium). For 12 day and 16 day mice, 50 μL and 100 μL liquid were gavaged, respectively; for the rest, 150 μL was gavaged. Pups with a bodyweight near the average level were selected for experiments before the first gavage. The mice in each group came from at least three dams and housed in at least 2 cages (n = 2–3 per cage) to avoid the cage-effect. Pups were separated from their mothers at 21 d of age and female and male pups were housed together. At 30 d of age (2 d after the last gavage), mice were killed and bacterial and tissue samples were collected for analysis.

As female and male pups were housed together throughout the 30 day experiment in Study 1, their GM composition was analyzed together here. Quantitative PCR (qPCR) using 16S universal or ITS1 primers[20] (Table S1) showed no significant differences in the bacterial counts or fungal loads of the intestinal samples among all groups, suggesting that the overall microbial loads were not influenced by LDP (Figures S1A and S1B). Nonetheless, significant differences were found in the bacterial compositions of the ileal mucosal ($p < 0.01$, Adonis test) and colonic luminal ($P < 0.001$ Adonis test) samples of the LDP and Ctr mice, as shown by weighted UniFrac distance measurements (Figures 1B and 1C). Notably, there was no significant difference between Ctr and F and P mice (Figures 1B and 1C), suggesting that both FMT and probiotics treatments efficiently restored the overall bacterial composition of these two intestinal regions. Similar trends were also found in the ileal lumen and colonic mucosa as shown by the difference of PC1 in Figures S1F to S1I.

We then analyzed the influence of LDP on OTUs based on Linear discriminant analysis Effect Size (LEfSe). LDP treatment mainly resulted in a reduction in *Lactobacillus* and *Candidatus Arthromitus* (segmented filamentous bacteria (SFB)) in all examined intestinal regions (Figures 1D and S1C–S1E). It is also worth noting that a more broad difference was observed between the ileal samples of the LDP and Ctr mice than that in colonic samples (Figures 1D and S1C–S1E).

Next, we evaluated the efficiency of FMT and probiotics on restoring these two bacterial taxa. Based on the 16S rDNA sequencing data, FMT efficiently restored the intestinal levels of both SFB and *Lactobacillus*, while the probiotics treatment, as expected, only restored *Lactobacillus* (Figures 1E and

1F). Moreover, three days after every gavage (i.e., one day before the next gavage) and at the end of (30 d) the study 1, the fecal and (or) intestinal levels of SFB and two treating probiotics (*L. bulgaricus* and LGG) were also determined by qPCR using species-specific primers (Table S1) and similar results were obtained as compared to the 16S rDNA sequencing data (Figure S1J). These results indicate that at least during the treatment period (from 12 d to 30 d of age), the intestinal SFB and (or) *Lactobacillus* levels were consistently affected by LDP, FMT and probiotic treatment.

In conclusion, LDP disturbed the intestinal bacterial composition, including a significant reduction in SFB and *Lactobacillus*, which was fully (for FMT) or partially (for probiotic) restored by several FMT and probiotic treatments.

LDP treatment persistently dampened intestinal IgA response

Early-life high-dose antibiotic treatment has been shown to transiently inhibit the intestinal IgA response in mice [17-18]. As intestinal SIgA is closely related to the development of MetS [21], we then sought to determine the influence of early-life LDP on intestinal IgA response. There were no significant difference in the fecal SIgA among all 14 d and 21 d age of mice, suggesting that the passive SIgA received from their mothers via breast milk was not influenced by LDP (Figure S2A). Nonetheless, in both 30-d-old male and female pups, when mice were able to actively generate intestinal SIgA [6], LDP tended to decrease the SIgA levels in ileal, caecal and colonic contents, which was (partially) restored by FMT and probiotic (Figures S2B, S2C, S2E, and S2F). However, because the small number (n = 2) of female pups in Ctr group of Study 1, we were not able to obtain statistically significant comparison results.

To further verify as well as determine the long-term effects of LDP on intestinal IgA response, we performed mouse Study 2 (Figure 2A). In this study, all the LDP, FMT, and probiotic treatments during early life were the same to Study 1, but the experimental period was extended to 25 weeks. And as a western diet (45% energy from lard) has been shown to accelerate the metabolic effects of LDP [3], the diet of mice was changed to a western diet at 6 weeks of age. In addition, a high-dose penicillin [HDP, 1.5 g/L (according to the recommended dose of penicillin for children [22]) in drinking water from 17 to 24 d of age] group was added to study the difference in intestinal IgA response between therapeutic and sub-therapeutic antibiotics. At 30 d of age, parts of pups were killed for the analysis of serum and intestinal (S)IgA and IgA-related lymphocytes. At 5, 10, 16, and 25 weeks of age, feces were collected to analyze the SIgA levels (Figure 2A).

Consistent to the previous studies [17-18], a decrease in fecal SIgA upon transient HDP treatment was found in 5- and 10-week-old mice (Figure 2B). This effect was disappeared, however, in 16- and 25-week-old mice (Figure 2B). Nonetheless, transient LDP reduced fecal SIgA throughout the 25-week experiment, showing a more persistent influence on SIgA than HDP (Figure 2A). Determination of caecal SIgA at 30 d and 25 weeks of age also obtained consistent results (Figure 2C). The reduction in intestinal SIgA upon LDP treatment was fully restored by FMT but only partially by probiotics (Figure 2A and 2C). In addition

to the intestinal SIgA, a moderate reduction in serum IgA was observed in LDP and HDP mice at 30 d of age as compared to that in Ctr, F and P mice, which, however, was disappeared at 25 weeks of age (Figure S2D).

Determination of the ileal IgA-producing antibody-secreting cells obtained consistent results (Figures 2D–2G and S3A–3D). In 30-d-old females, LDP decreased the absolute numbers of IgA+ plasma cells (PCs, IgA+ B220-) within the distal small intestine lamina propira (SLP) and Peyer's patches (PPs) (Figures 2D and 2F). A reduction in the numbers of IgA+ B cells (IgA+ B220+) was also found in SLP but not PPs (Figures 2D and 2F). The inhibition of IgA+ antibody-secreting cells (ASCs) within SLP (but not PPs) by LDP was also observed in 25-week-old mice, suggesting a persistent effect (Figures 2E and 2G). The inhibition of IgA-producing ASCs by LDP was also fully or partially restored by FMT and probiotics (Figures 2D–2E). With respect to LDP, a stronger inhibition of IgA+ ASCs within SLP and PPs by HDP was observed in 30-d-old females; however, this inhibition was transient and disappeared in 25-week-old females (Figures 2D–2G). Similar results were also obtained from males (Figures S3A–S3D).

We then sought to determine the possible cause(s) contributing to the differences in SIgA production between LDP and HDP. Previous studies have shown that high-dose antibiotic treatment around weaning persistently reduced the ileal regulatory T cells (Tregs) in mice [23], a subgroup of which, RORγ+ Tregs, have been shown to inhibit the generation of intestinal SIgA [24]. Consistent to these results, we found that HDP reduced the SLP Tregs at both 30 d and 25 weeks of ages, while LDP had no significant influence on SLP Tregs (Figures S3E–S3L). Further determination of RORγ+ Tregs subgroup obtained similar results (Figures S3E–S3L). These results suggest that a reduction in Tregs, especially RORγ+ Tregs, may therefore counteract the long-term inhibition of HDP on SIgA production [24].

Conclusively, with respect to the relatively short-term inhibition of intestinal IgA response by HDP, transient LDP during early life persistently dampened intestinal IgA response and reduced IgA production, which could be lasted for at least for 25 weeks. Moreover, this LDP-induced effect on intestinal IgA response could be (partially) restored by several times of FMT or probiotic treatments.

The inhibition of intestinal IgA response by LDP was GM- and early life-dependent

As intestinal IgA response is greatly dependent on the colonization and composition of GM [25-26], we then sought to determine the correlation between LDP-induced changes in GM and inhibition of intestinal IgA response.

We firstly examined the *in vitro* IgA-inducing capabilities of the antigens derived from the feces of 21-d-old mice in Study 1 as previously described [7, 27]. Briefly, antigens separated from the feces through centrifugation were normalized and co-cultured with ileum tissue samples (containing no visible PPs) obtained from 8-week-old SPF C57/BL6 mice to study the effects of these antigens on ileal IgA production. After 2 d of cultivation, the ileum tissue produced significantly more IgA when co-cultured

with antigens derived from the feces of Ctr and F mice than from LDP mice (Figure 3A). A similar trend was evident for the antigens from the feces of P mice compared to the LDP mice but did not reach significance (P = 0.094). Moreover, the mRNA expression of the *Jchain* and *IL-6* of the ileum tissue was also higher, while tumor necrosis factor (ligand) superfamily, member 13 (also known as APRIL) and 13b (also known as BAFF) were not influenced, when cultured with antigens derived from the feces of Ctr and F mice than those from the LDP mice (Figure 3B), suggesting that Ctr and F antigens may increase IgA production through enhancing the survival and activity of IgA+ PCs [19].

These results suggest that LDP inhibit the intestinal immune response to GM, RNA-sequencing of the ileum from 30-d-old mice in Study 1 confirmed these results. Several biological functions related to IgA production and immune response to microbes that were downregulated in the LDP mice compared to the Ctr, F, and P groups, including PI3K signaling in B lymphocytes, B cell receptor signaling, dendritic cell maturation, and Th1 and Th17 pathways (Figure 3D).

To further determine the correlation between LDP-induced changes in GM and IgA production, we transferred fecal microbiota from 30-d-old mice in Study 1 to even-aged male germ free (GF) mice, and measured the fecal SIgA levels in recipients. Three weeks post-transfer, LDP recipients (LDPR) exhibited significantly lower fecal SIgA levels compared to that of Ctr recipients (CtrR) and F recipients (FR), as well as the P recipients (PR) (Figure 3C). The difference in the fecal SIgA levels of the LDPR, CtrR, FR, and PR lasted 6 weeks after the transfer (Figure 2C). However, contrary to the donors, the fecal SIgA differences disappeared 12 weeks after the transfer (Figure 3C), suggesting that the time factor (early life) also play an important role in the prolonged influence of LDP-induced GM alteration on IgA responses. Moreover, no significant difference in serum IgA 12 weeks after transfer was observed among all recipients (Figure 3C).

Together, these results indicated that LDP-induced changes in GM mediated the inhibition of intestinal IgA response and that early life is critical for the long-lasting effects of LDP on intestinal IgA response.

LDP induced persistent changes in the ileal microbiota in a SIgA-dependent manner

As intestinal SIgA is a master controller of the GM, we then sought to determine the effects of LDP-induced decrease in SIgA on GM. To this end, we performed Study 3 (Figure 4A) using SIgA-deficient (*Pigr*$^{-/-}$) mice generated by *Pigr*$^{+/-}$ females and males. The LDP, FMT and probiotic treatments were the same to Study 1 but the experimental period was extended to 25 weeks. All mice were transferred to a western diet (45% energy from lard) at 6 weeks of age and lasted to the end of the experiment to accelerate the effects of LDP [3]. In addition, due to the insufficient number of male *Pigr*$^{-/-}$ pups, only female *Pigr*$^{-/-}$ pups were selected for the experiment at 10 days of age.

We firstly analyzed the fecal, serum, and caecal (S)IgA levels. Before weaning, no significant difference in fecal SIgA was observed between WT (*Pigr*$^{+/+}$ and *Pigr*$^{+/-}$) and *Pigr*$^{-/-}$ pups while higher fecal SIgA levels

were found in WT pups after weaning (Figure S4A). In 25-week-old mice, there was no significant difference in serum IgA among all groups in both WT and *Pigr*$^{-/-}$ mice (Figure S4B). However, a moderate (P = .065) increase in serum IgA was found in *Pigr*$^{-/-}$ as compared to WT females (Figure S4D). In consistent to the results found in Study 1, LDP decreased the caecal SIgA levels in 25-week-old WT mice, which was (partially) restored by FMT and probiotics (Figure S4C). In addition, no significant difference in serum and fecal (S)IgA was found between the WT mice of two genotypes (*Pigr*$^{+/+}$ and *Pigr*$^{+/-}$) (Figure S4E).

We then analyzed the influence of LDP on GM in Study 3. No significant difference in fecal bacterial composition was observed between 21-d-old *Pigr*$^{-/-}$ mice and their WT littermates (Figure S4G), suggesting that the starting GM was not influenced by the genotypes. At 25 weeks of age, WT LDP females showed a significantly different bacterial composition in the ileal but not colonic mucosa compared to WT Ctr females (Figures 4B and S4H, Adonis test), which was in line with previous study showing a more closely interaction between SIgA and ileal microbiota [28]. Similar difference was found for WT males but did not reach significance (P = 0.082) (Figure 4C, Adonis test). Moreover, FMT (moderately) restored this LDP-induced changes in ileal mucosal microbiota in WT mice (Figures 4B and 4C). In contrast to WT mice, no significant difference in the ileal bacterial composition were found among all groups in *Pigr*$^{-/-}$ mice (Figure 4D, Adonis test), suggesting that intestinal SIgA may mediate this long-term effects of LDP on ileal microbiota.

To further verify this assumption, we performed mouse Study 4 using B cell-deficient (μMT) mice (Figure 4A). Briefly, pan B cells (including PCs) isolated from the spleens, PPs, mesenteric lymph nodes and ileal and colonic lamina propria of 30 day LDP-treated (LDP, F, and P groups) or -free (Ctr) WT SPF mice were purified and adoptively transferred to even-aged μMT mice. After transfer, mice were housed 2–3/cages (2 cages for each group) to avoid the cage-effect. Twelve weeks after the transfer, recipients were killed for GM analysis. B cells were successfully colonized in the recipients, as considerable SIgA was detected in the caecal contents except for recipients received PBS treatment (Figure S4F). As expected, we found a moderate (P = 0.143, Adonis test) difference in the ileal microbiota between Ctr and LDP recipients while a significant difference was found between LDP and F recipients (Figure 4E, Adonis test). In addition, PBS recipients showed a significant difference in the ileal microbiota compared to all other B cell-received recipients (Figure 4E, Adonis test).

Collectively, we demonstrated that transient LDP during early life can induce persistent changes in the ileal microbiota in an intestinal SIgA-dependent manner, which could be (partially) restored by FMT and probiotics.

LDP-induced reduction of SIgA increased bacterial encroachment and adipose inflammation

Intestinal SIgA can bind to the microbial antigens, preventing bacterial encroachment and adhesion to intestinal epithelial cells (IECs) as well as the translocation of bacteria and their metabolites, such as lipopolysaccharides (LPS) and flagellin, therefore protecting hosts from inflammation [19]. We then sought to investigate the influences of LDP-induced reduction in intestinal SIgA on bacterial encroachment and inflammation in 25-week-old mice from Study 3.

As expected, confocal microscopy, using mucus-preserving Carnoy fixation [29], showed that WT LDP females exhibited reduced distance between the bacteria and IECs, and showed exaggerated bacterial translocation into the in the distal ileum as compared to Ctr females, which was restored in FMT and P females (Figures 5A and 5B). An enhanced bacterial translocation was observed in *Pigr*$^{-/-}$ mice than WT mice while no significant difference was observed among all *Pigr*$^{-/-}$ mice (Figures S5C and S5D). In consistent to this, a decrease in IgA+ bacteria in ileum was observed in LDP females as compared to that in Ctr, F, and P females (Figures 5C and 5D). This compromised control of bacteria by SIgA was accompanied with an increase in serum LPS in WT but not *Pigr*$^{-/-}$ LDP females as compared to that in Ctr, F, and P females with identical genotypes (Figure 5E), while no significant difference in serum TNF-α and IL-6 was observed among all groups (Figures S5M and S5N).

We then determined the influence of LDP on adipose inflammation, a key factor involved in the development of insulin resistance [30]. A significant increase in macrophage infiltration in visceral adipose tissue, an indicator of adipose inflammation, was found in WT LDP females compared to that in WT Ctr females, as determined by immunostaining of F4/80 (Figures 5F and 5G). Gene expression analysis using qPCR also demonstrated increases in the mRNA expression of TNF-α and IL-6 in the visceral adipose tissue of WT LDP females than that of WT Ctr, F, and P females (Figures S6E and S6F). This LDP-induced adipose inflammation was disappeared in *Pigr*$^{-/-}$ females (Figure S6).

With respect to WT females, similar influences of LDP and FMT treatments on bacterial encroachment and adipose inflammation were observed in WT males, while a moderate influence of probiotics was found (Figures S5 and S6). Collectively, transient exposure to LDP during early life caused increases in ileal bacterial encroachment and adipose inflammation in a SIgA-dependent manner, which could be (partially) counteracted by FMT and probiotic treatments.

Dysbiosis and bacterial encroachment enhanced the development of inflammation and MetS

Previous studies have shown that LDP can enhance the development of MetS, however, the mechanism(s) and the therapies were poorly determined [3, 16]. Considering an essential role of intestinal SIgA in controlling the GM and MetS [21], and the above results showing that intestinal SIgA mediated the LDP-induced increases in inflammation, a key factor contributing to MetS, we speculated that LDP-induced decreases in intestinal SIgA may also mediated the enhancement of MetS. To verify these

assumptions, we measured the parameters related to MetS, including body weight (BW), fat mass (rate), serum hormones and glucose, and insulin sensitivity, in 25-week-old WT and *Pigr*$^{-/-}$ mice in Study 3.

LDP enhanced the development of western diet-induced MetS in WT females, including increases in BW, fat and adipocyte tissues masses, adipocytes size, hepatic triglyceride, and serum glucose, insulin, and leptin levels (Figures 6A–6F, S7C and S7D). In consistent to the elevated fast serum glucose and insulin, glucose and insulin tolerance tests also showed impaired glucose tolerance and insulin sensitivity in LDP females as compared to that in Ctr females (Figures S7G and S7H). In addition, LDP decreased the serum levels of peptide YY (PYY), an GM-related anti-obesity peptide secreted by L cells in the gastrointestinal tract [31]; while increased serum insulin-like growth factor-1 (IGF-1), a hormone secreted by the liver and intestine that can promote growth and preadipocyte proliferation and is also closely linked to obesity and the GM [32-33] (Figure 6G). Similar effects of LDP on the metabolism were also observed in WT males (Figures 6 and S7). Moreover, FMT and probiotic treatments counteracted the LDP-effect on the development of MetS to different degrees: a more profound influence was found upon FMT treatment compared to probiotics (Figures 6 and S7).

Lastly, in contrast to the WT mice, no significant difference in these parameters was found among all groups in their female *Pigr*$^{-/-}$ littermates, demonstrating an indispensible role of intestinal SIgA in mediating LDP-induced effects on the development of MetS (Figure S8).

Discussion

In this study, we showed that the LDP treatment during early life disturbed GM composition, resulting in a persistent inhibition of the intestinal IgA response and decrease in intestinal SIgA, which led to a disruption in the ileal bacterial composition, increases in bacterial encroachment and adipose inflammation, and an enhancement of diet-induced MetS. Several FMT or probiotic administrations during the LDP treatment period fully (FMT) or partially (probiotics) restored the intestinal IgA levels and prevented LDP-induced MetS.

The intestinal mucosal GM is more stable and resistant to disturbance factors than the luminal GM [34]. In line to this, we found that transient LDP exposure disturbed both the mucosal and luminal GM in 30-d-old WT mice while only the ileal mucosal GM was still altered by LDP in 25-week-old WT mice. This persistently influence on ileal microbiota by LDP is mediated by the intestinal SIgA as the ileal microbiota was not affected by LDP in their even-aged SIgA-deficient (*Pigr*$^{-/-}$) littermates. The uneven distribution of SIgA-producing ASCs and SIgA in the intestine may also contribute to the different influences of LDP on GM between the ileum and colon as well between lumen and mucosa: (1) The distal small intestine (including the PPs) is the main inductive and effective site of IgA+ B cells, which is also the main place where the interaction between SIgA and GM taking place [28, 35]; and (2) the intestinal mucosa has a higher SIgA level than the lumen [19].

The intestinal IgA+ B cell repertoire can be greatly shaped by the routine of GM colonization in GF mice [36]. Although this has not been verified in the newborn mice, considering their similarities (both firstly experience a GM-induced intestinal IgA+ B cells differentiation and maturation), similar mechanisms may be also the same with newborns. This influence on IgA repertoire can last for a long time, which may be partially attributed to the long-living property of IgA+ B cells [37-38]. In line to this, we found that transient changes in GM (as observed in *Pigr*$^{-/-}$ mice) during early life led to a persistent inhibition of intestinal IgA response. In addition, our results also demonstrated that IgA+ B cells differentiation in newborn mice is more sensitive to GM alteration than that in GF mice, since the intestinal SIgA reduction continued until the end of the experiment (25 weeks) in the WT SPF mice (whose GM was disturbed since birth) but disappeared in conventionalized GF mice (received GM at 30 d old) 12 weeks after the GM transfer.

It has been previously demonstrated that transient early-life exposure of high-dose antibiotics induced a similar inhibition of intestinal IgA response and decrease in intestinal and serum (S)IgA to LDP [17-18]. However, in contrast to the persistent (at least for 25 weeks) effect of LDP on intestinal IgA response as observed in our study, high-dose antibiotics only show a transient (up to 10 weeks) effect on the fecal SIgA, which was also verified by our results (Figure 2B). Through determination of cells related to intestinal IgA response using flow cytometry, we found a decrease in the total and RORγ+ Tregs within the SLP in mice of both 30 d and 25 weeks of age upon LDP treatment (Figure S3). This decrease in RORγ+ Tregs, which has been previously shown to be inversely correlated with the intestinal SIgA [24], may therefore contribute to the restoration of intestinal SIgA levels in HDP mice. In addition, the treating time of HDP may be also important. In this study, we treated the mice with HDP around weaning (from 17 d to 24 d of age). This is a critical time when a so-called “weaning action” has a fundamental influence on the later-life intestinal immunity [23]. Elimination of the GM by high-dose antibiotics during this time can disturb this process and persistently impairing the intestinal immunity, including a reduction in Tregs [23], as observed in our study (Figure S3). Therefore, more works are warranted to further determine the time factor of high-dose antibiotics on the intestinal IgA response and its contribution to the observed difference in the intestinal IgA response between HDP and LDP.

A major role of intestinal SIgA is enhancing the clearance of microbes and preventing the encroachment and translocation of microbes and microbial antigens, therefore protecting the hosts from microbes-induced inflammation [21]. In accord, we found that the transient LDP-induced dampen of intestinal IgA response increased bacterial encroachment and translocation and serum LPS, which was accompanied with an exacerbation of adipose inflammation. A compromise of the intestinal IgA response has also been reported in high-fat diet (HFD)-induced obese mice [39]. In addition, deficient in IgA (*Igha*$^{-/-}$) exacerbates the HFD-induced adipose inflammation and MetS in mice [39] while an enhancement of IgA response through flagellin immunization can prevent HFD-induced MetS in a B and CD4+ T cells-dependent manner [40]. However, as both systemic (serum IgA) and mucosal SIgA were lack in *Igha*$^{-/-}$ and μMT mice, it is not clear which kind of IgA plays a major role in regulating metabolism by these studies [39-40]. We found that although LDP exposure reduced both the serum IgA and intestinal SIgA in 30-d-old WT mice, only the intestinal SIgA was still affected by the LDP in 25-week-old WT mice. In addition,

through using SIgA-selectively deficient mice (*Pigr*$^{-/-}$), we demonstrated that only mucosal SIgA, especially the intestinal SIgA, had a fundamental role in mediating LDP-induced alteration in the GM and metabolism.

In addition, FMT and probiotics are both interventions with certain effectiveness to improve LDP-induced MetS. Although FMT is more efficient than probiotics, finding proper donors, as well as the acceptability and safety (especially for infants), are significant issues that need to be addressed. Probiotics are safer and more acceptable than FMT but exhibit lower efficiency. Additionally, the initiation and duration times, as well as the dosage level and frequency, are factors that should be considered. Moreover, future studies should focus on the differences between FMT and probiotics (such as the efficiency of SFB restoration in mice) and seek efficient and safe ways to treat Abx-induced MetS.

Conclusions

Transient LDP exposure during early life disturbed the intestinal bacterial composition in mice, which led to a persistently dampen of intestinal IgA response. Reduction in SIgA mediated the persistently influences of LDP on ileal microbiota, accompanied by increases in bacterial encroachment and translocation and adipose inflammation, enhancing the development of diet-induced MetS.

Methods

Animals

Wild-type specific pathogen free animals

Wild-type (WT) C56BL/6J mice purchased at 8 weeks of age (Vital River Laboratory Animal Technology. Co., Ltd., China) were randomly paired (1:1) after adapting for one week and fed a standard diet (#12450B, Research Diets). After cohousing for 4 days (one estrous cycle for house mouse), females were separated from the males and fed solely. During and after cohousing, pregnancies and due dates were monitored and calculated according to the body weight changes.

Pups (and their mothers) were randomly assigned to four groups: (1) low-dose penicillin (LDP)-free control group (Ctr) that received no antibiotics, (2) LDP-treated control group (LDP) that received antibiotics only, (3) FMT-treated group (F) that received LDP and fecal microbiota transplantation treatments, and (4) probiotics-treated group (P) that received LDP and probiotic cocktail treatments. Pups were separated from their mothers at 21 days. Pups in every group were from at least three dams and born within 24 hours. Pups in the Ctr and F groups were born within 24 hours. For the LDP, F and P groups, dams received antibiotics at a dose of 10 mg/L to deliver approximately 1.5 mg per kg body weight about one week prior to birth and were continuously maintained on penicillin [3]. Pups in the three groups were exposed to penicillin until 30 days of age either through their mother or through drinking water. After the LDP treatment, pups were divided by sexes and kept 2~3/cages. Pups in the F and P groups were gavaged with fecal microbiota from Ctr and probiotics, respectively at 12, 16, 20, 24 and 28

days of age. For the FMT group, feces were collected from pups in the Ctr group, pooled, and immediately placed in prereduced anaerobically sterilized PBS (0.3 g feces/mL PBS), homogenized under anaerobic conditions, settled with gravity for 2 minutes, and then the supernatant was transferred to pups in the F group. For the P group, pups were gavaged with prereduced anaerobically sterilized PBS containing *Lactobacillus bulgaricus* and *Lactobacillus rhamnosus* GG at ~10^8/mL for each bacterium. For the Ctr and LDP groups, pups were gavaged with prereduced anaerobically sterilized PBS on the same days. For 12 day and 16 day mice, 50 μL and 100 μL liquid were gavaged, respectively; for the rest, 150 μL was gavaged. All pups were fed on normal diet (#D12450B, Research Diets) but transferred to a western diet (45% energy from lard, #D12451, Research Diets) at 6 weeks of age and allowed *ad libitum* access to food and water.

Germ-free animals

For the microbiota transfer to germ-free (GF) animals experiment, feces were collected from 30-day-old donors from each group and immediately placed in prereduced anaerobically sterilized PBS, homogenized under anaerobic conditions, settled with gravity for 2 minutes, and then the supernatant was transferred to even-aged GF C57BL/6 mice (n = 8 for each group, n (females) = n (males) = 4). After transfer, the conventionalized GF mice were housed in standard SPF conditions, and food and water were provided *ad libitum*.

SIgA-deficient mice

Pigr$^{+/-}$ males and females, which can produce normal SIgA and therefore have similar GM to WT mice[6], were used to generate SIgA-deficient pups. Specifically, 8-week-old *Pigr*$^{+/-}$ females and males were mated as above specified, genotypes of pups were identified at 10 days of age and only *Pigr*$^{-/-}$ female and WT mice pups were chosen for the following experiment as specified above.

B cell-deficient (μMT) mice

Separation and transfer of pan B cells to B cell-deficient (μMT) mice was conducted as previously described with some modification [39]. Pan B cells (includes plasma cells) from the spleens, Peyer's patches, mesenteric lymph nodes and ileal and colonic lamina propria of 30 day LDP-treated or -free WT SPF mice were purified using negative selection (>90% purity, EasySep; StemCell Technologies) and injected intraperitoneally (~5.5×10^6 cells) in even-aged μMT mice.

Animal management and sampling

Mice were housed in standard specific pathogen-free (SPF) conditions (12/12-hour light-dark cycle, humidity at 50 ± 15%, temperature of 22 ± 2°C), and food and water were provided *ad libitum*. The food used in this study was sterilized using radiation (25.0 kGy). Food intake was recorded every week. Body weight was recorded weekly. At the end of the experimental period, the mice were fasted for 12 hours, and plasma was collected by eyeball extirpation. The lumen contents of the distal ileum and proximal colon

were collected by washing the lumen with sterilized PBS, and the mucosal samples were collected by scraping the intestinal wall with sterilized glass slides. Then, the samples were stored at -80°C for microbial analysis. The contents of the cecum were collected and stored at -80°C for the analysis of secreted IgA (SIgA). The weights of the liver, inguinal white adipose tissue (iWAT), epididymal white adipose tissue (eWAT) and mesenteric white adipose tissue (mWAT) were measured. Tissues were preserved at -80°C for gene expression analysis (for ileum, all fat and mesentery were removed, and Peyer's patches were excised from the ileum), and the liver, iWAT, colon and ileum were fixed using 4% paraformaldehyde and used for hematoxylin-eosin (H&E) staining, immunofluorescence and immunohistochemistry analysis.

The guidelines of the institute regarding the care and use of laboratory animals were followed. This study was approved by the Animal Experiment Committee of the College of Food Science and Nutritional Engineering at China Agricultural University.

Ileum tissue culture

Mouse ileum was obtained and cultured as previously described with some modification [27]. Distal ileum samples containing no Peyer's patches were washed and cultured using RPMI 1640 supplemented with 10% FCS and penicillin/streptomycin 50 mg/ml at 37°C and 5% CO2 in 24-well plates. Two ileum samples per well (~ 3 mm) were cultured for each group (n = 4). Two days after co-culture with antigens, culture medium was collected and supernatants were centrifuged and stored at -80°C for the analysis of IgA and cells were collected for the analysis gene expression. Four eight-week-old male SPF C57/BL6 mice were used for sampling. The ileum samples of each group were taken from all four mice and comprised the same intestinal regions.

Isolation and analysis of immune cells from the intestine

lymphocytes from the intestinal lamina propira (LP) and Peyer's Patches (PPs) were isolated by adapting a method as previously described[39]. Distal ileum (~10 cm prior to the cecum) was extracted, removing all mesentery fat as possible and PPs, and collected in ice-cold harvest media (RPMI 1640 (Sigma) supplemented with 5% FBS (Gibco), 15 mM HEPES, Penicillin-Streptomycin (Gibco), pH 7.4). Extracted intestines were cut open longitudinally into 2~3 mm pieces in the wash buffer. Bowel pieces were transferredto an EDTA-containing stripping buffer (Hank's balanced salt solution (Gibco) supplemented with 2% FBS (Gibco), 1.3 mM EDTA, 15 mM HEPES, Penicillin-Streptomycin (Gibco), pH 7.4) and shaken vigorously at 37 °C for 20 min, and then vortexed gently for a few seconds. This step was repeated for two times. Gut pieces were then washed in cold harvest medium to remove residual EDTA before transfer into a digestion buffer (RPMI 1640 supplemented with 10% FBS (Gibco), 10 mM sodium pyruvate, penicillin–streptomycin antibiotics (Gibco), 15 mM HEPES, collagenase type I (100 U/mL, Sigma), DNase I (0.5 mg/mL, Sangon), and 1 mM $CaCl_2$ and $MgCl_2$), where it was minced finely with scissors, followed by a 45 min incubation at 37 °C with shaking. The resulting suspension of LP immune cells collected

from the previous step were filtered twice through a 100- and 40-μmnylon cell strainer to obtain a single-cell suspension. PPs were mechanically disrupted in the harvest medium and the homogenate was filtered through a 70 μm cell strainer to obtain a single-cell suspension. Single-cells were stimulated with 50 ng/mL phorbolmyristate acetate and 1 μM Ionomycin in the presence of 5 μg/mL Brefeldin A. Following the stimulation. Following this in vitro stimulation, cells were stained with Fixable Viability Stain 780 (BD), anti-CD45.2, anti-CD4, anti-CD19, anti-CD45R and anti-Tcrβ before fixed and permeabilized using Transcription Factor Buffer (BD Pharmingen). After fixation and permeabilization, cells were further stained with anti-IgA, anti-Foxp3, and anti-RORγ amtibodies. Cells were acquired on an LSRFortessa^{TM} Cell Analyzer (BD) and analyzed with FlowJo (Tree Star, Ashland) software.

Quantitative Real-time PCR (qPCR) Analysis

Total RNA was extracted using TRIzol^{TM} reagent (Invitrogen) according to the manufacturer's instructions. Reverse transcription of the total RNA (2.5 μg) was performed with a high-capacity cDNA reverse transcription kit (Promega Biotech Co., Ltd). qPCR was run in triplicate for each sample and analyzed in a LightCycler 480 real-time PCR system (Roche). Data were normalized to the internal control *β-actin* and analyzed using the △△CT method. The expression of genes in iWAT, the liver, ileum and colon, as well as the bacterial and fungal load, were determined through qPCR (the related genes and primers used are shown in Table S1).

Quantification of the bacterial and fungal loads through qPCR was conducted as previously described[41]. Briefly, the total bacterial DNA was isolated from the samples with a QIAamp DNA Stool Mini Kit (Qiagen) following the manufacturer's instructions. For the isolation of fungal DNA, samples were suspended in 50 mM Tris buffer (pH 7.5) supplemented with 1 mM EDTA, 0.2% b-mercaptoethanol and 1000 units/ml of lyticase (Sigma), incubated at 37°C for 30 min to disrupt fungal cells as described[42], prior to processing through the QIAamp DNA Stool Mini Kit (Qiagen). The DNA was then subjected to qPCR using a QuantiFast SYBR Green PCR kit (Bio-Rad) with specific primers (Table S1).

Determination of Body Composition through MRI

MRI experiments were performed on 30-day-old and 25-week-old mice. The body composition was determined using MesoQMR instrument (Testniumag, Shanghai, China) with a 60 mm receiver and 0.5 ± 0.08 T magnetic field strength. To obtain high resolution scanned MRI images, MRI measurements were performed on a 7.0 T Varian MRI instrument (Varian Medical Systems, Palo Alto, CA, USA) using a 40 mm volume and receiver coil at the Institute of Laboratory Animal Sciences, Chinese Academy of Medical Sciences. Prior to the experiments, the mice were initially anesthetized with 2% isoflurane in a dedicated chamber. During the course of MRI, anesthesia levels were reduced to 1.5–1% in a combination of medical air and medical oxygen. The mice were positioned in the prone position, and respiratory-gated image acquisition was performed. MRI images of the mice were analyzed by Argus software.

Plasma Biochemical Parameters

The plasma biochemical parameters, including, glucose, cholesterol and triglyceride (TG) levels, were determined by a 3100 Clinical Analyzer (Hitachi High-Technologies Corporation, Japan).

Quantification of Serum Hormones and SIgA

Serum leptin, insulin, PYY, IGF-1, and IgA, as well as intestinal/fecal SIgA levels were determined using ELISA kits (Sangon Biotech, Shanghai, China) according to the manufacturer's recommendations.

Separation of antigens and determination of IgA to the specific antigens were conducted as described with some modification[7, 40]. Briefly, to prepare antigens from cecal contents of mice carrying GM composed of "pure or none Firmicutes", cecal contents of mice from each group were normalized by bacterial loads (determined by qPCR as previously described[20]), pooled (n = 3) in PBS (sterilized with a 0.22 μm filter), vortexed for 5 min, and centrifuged for 5 min at 13000 RPM, 4°C. Samples were then sonicated for 15 min and centrifuged for 15 min at 13000 RPM, 4°C. Supernatant was taken and protein was measured using BCA assay (Thermo Fisher). For the determination of IgA to specific antigens, 96-well microtiter plates (Costar, Corning, New York) were coated with 1 mg/ml of antigen in 9.6 pH bicarbonate buffer overnight at 4 °C, then IgA from the cecal contents of 30 day or 25 week mice were loaded at 1:20 dilution for 1 h at 37°C. Anti-IgA Biotin and HRP Conjugated Streptavidin were used to detect binding of IgA.

Immunofluorescence and immunohistochemistry

Tissue sections for immunohistochemical testing were prepared on poly-L-lysine-pretreated coverslips. Immunohistochemical staining was performed according to a standard protocol using antibodies against F4/80 at a 1:200 dilution. The samples were incubated overnight in a humidified chamber at 4°C. Secondary antibodies for immunohistochemical staining were purchased from Invitrogen. All images were acquired on an Olympus BX51 system and processed using ImageJ software, version 1.8.0. Immunostaining for IgA was conducted using FITC-conjugated anti-IgA antibody at a 1:500 dilution. The samples were incubated overnight at 4°C. Observations and analyses were performed with a Zeiss LSM 700 confocal microscope.

Localization of bacteria by fluorescent in situ hybridization

The localization of bacteria by fluorescent in situ hybridization (FISH) was conducted as previously described with some modifications [29]. Briefly, distal ileum (second cm from the caecum) containing fecal material was placed in methanol-Carnoy'sfixative solution (60% methanol, 30% chloroform, 10% glacial acetic acid) for a minimum of 3 h at room temperature. The hybridization step was performed at 50 ℃ overnight with an modified EUB338 probe [43] (EUB338-II, 5'-GCAGCCACCCGTAGGTGT-3', with a 5' Texas

Red label) diluted to a final concentration of 10 mg/ml in hybridization buffer (20 mM Tris-HCl, pH7.4, 0.9 M NaCl, 0.1% SDS, 20% formamide). After washing, Mucin 2 primary antibody was diluted to 1:500 in block solution and applied overnight at 4 ℃. After washing, block solution containing anti-rabbit FITC-conjugated secondary antibody diluted to 1:1000 was applied to the section for 2 h. After washing, slides were mounted using Prolong anti-fade mounting media (Life Technologies). Observations were performed with a Zeiss LSM 700 confocal microscope with software Zen 2011 version 7.1. This software was used to determine the distance between bacteria and the epithelial cell monolayer.

Histology

Tissues fixed in 4% paraformaldehyde were cut into 5 μm sections after being embedded in paraffin. Multiple sections were prepared and stained with hematoxylin and eosin (H&E) for general morphological observation.

GM Analysis

The microbial community of fecal, mucosal and lumen samples of colon and ileum were analyzed through the sequence of 16S rRNA gene V4 region. Briefly, Total genome DNA from samples was extracted using CTAB/SDS method. DNA concentration and purity was monitored on 1% agarose gels. According to the concentration, DNA was diluted to 1 ng/μL using sterile water. 16S rRNA gene V4 region were amplified used specific primer for V4 region (515F-806R) with the barcode. All PCR reactions were carried out in 30 μL reactions with 15 μL of Phusion® High-Fidelity PCR Master Mix (New England Biolabs); 0.2 μM of forward and reverse primers, and about 10 ng template DNA. Thermal cycling consisted of initial denaturation at 98°C for 1 min, followed by 30 cycles of denaturation at 98°C for 10 s, annealing at 50°C for 30 s, and elongation at 72°C for 30 s. Finally 72°C for 5 min. Mix same volume of 1×loading buffer (contained SYB green) with PCR products and operate electrophoresis on 2% agarose gel for detection. PCR products were mixed in equidensity ratios. Then, mixture PCR products were purified with GeneJETTM Gel Extraction Kit (Thermo Scientific). Sequencing libraries were generated using Ion Plus Fragment Library Kit 48 rxns (Thermo Scientific) following manufacturer's recommendations. The library quality was assessed on the Qubit@2.0 Fluorometer (Thermo Scientific). At last, the library was sequenced on an Ion S5TM XL platform and 400 bp/600 bp single-end reads were generated.

Single-end reads was assigned to samples based on their unique barcode and truncated by cutting off the barcode and primer sequence. Quality filtering on the raw reads was performed under specific filtering conditions to obtain the high-quality clean reads according to the Cutadapt (V1.9.1, http://cutadapt.readthedocs.io/en/stable/) quality controlled process. The reads were compared with the reference database (Silva database, https://www.arb-silva.de/) using UCHIME algorithm (UCHIME Algorithm, http://www.drive5.com/usearch/manual/uchime_algo.html) to detect chimera sequences, and then the chimera sequences were removed[44]. Then the Clean Reads finally obtained.

Alpha diversity is applied in analyzing complexity of species diversity for a sample through 6 indices, including Observed-species, Chao1, Shannon, Simpson, ACE, Good-coverage. All this indices in our samples were calculated with QIIME (V1.7.0) and displayed with R software (V2.15.3). Beta diversity analysis was used to evaluate differences of samples in species complexity, Beta diversity on both weighted and unweighted unifrac was calculated by QIIME software (V1.7.0). Principal Coordinate Analysis (PCoA) was performed to get principal coordinates and visualize from complex, multidimensional data. A distance matrix of weighted or unweighted unifrac among samples obtained before was transformed to a new set of orthogonal axes, by which the maximum variation factor is demonstrated by first principal coordinate, and the second maximum one by the second principal coordinate, and so on. PCoA analysis was displayed by WGCNA package, stat packages and ggplot2 package in R software (V2.15.3).

RNA-sequencing

Total RNA of the liver and ileum were extracted using TRIzol^{TM} reagent (Invitrogen) according to the manufacturer's instructions. RNA degradation and contamination was monitored on 1% agarose gels; RNA purity was checked using the NanoPhotometer® spectrophotometer (IMPLEN, CA, USA); RNA concentration was measured using Qubit® RNA Assay Kit in Qubit®2.0 Flurometer (Life Technologies, CA, USA); RNA integrity was assessed using the RNA Nano 6000 Assay Kit of the Bioanalyzer 2100 system (Agilent Technologies, CA, USA). Then a total amount of 3 μg RNA per sample was used as input material for the RNA sample preparations. Sequencing libraries were generated using NEBNext® UltraTM RNA Library Prep Kit for Illumina® (NEB, USA) following manufacturer's recommendations and index codes were added to attribute sequences to each sample. Briefly, mRNA was purified from total RNA using poly-T oligo-attached magnetic beads. Fragmentation was carried out using divalent cations under elevated temperature in NEBNext First Strand Synthesis Reaction Buffer (5X). First strand cDNA was synthesized using random hexamer primer and M-MuLV Reverse Transcriptase (RNase H^-). Second strand cDNA synthesis was subsequently performed using DNA Polymerase I and RNase H. Remaining overhangs were converted into blunt ends via exonuclease/polymerase activities. After adenylation of 3' ends of DNA fragments, NEBNext Adaptor with hairpin loop structure were ligated to prepare for hybridization. In order to select cDNA fragments of preferentially 250~300 bp in length, the library fragments were purified with AMPure XP system (Beckman Coulter, Beverly, USA). Then 3 μL USER Enzyme (NEB, USA) was used with size-selected, adaptor-ligated cDNA at 37°C for 15 min followed by 5 min at 95°C before PCR. Then PCR was performed with Phusion High-Fidelity DNA polymerase, Universal PCR primers and Index (X) Primer. At last, PCR products were purified (AMPure XP system) and library quality was assessed on the Agilent Bioanalyzer 2100 system. The clustering of the index-coded samples was performed on a cBot Cluster Generation System using TruSeq PE Cluster Kit v3-cBot-HS (Illumia) according to the manufacturer's instructions. After cluster generation, the library preparations were sequenced on an Illumina Hiseq platform and 125 bp/150 bp paired-end reads were generated.

Raw data (raw reads) of fastq format were firstly processed through in-house perl scripts. In this step, clean data (clean reads) were obtained by removing reads containing adapter, reads containing ploy-N and low quality reads from raw data. At the same time, Q20, Q30 and GC content the clean data were calculated. All the downstream analyses were based on the clean data with high quality. Reference genome and gene model annotation files were downloaded from genome website directly. Index of the reference genome was built using Hisat2 (V2.0.5) and paired-end clean reads were aligned to the reference genome using Hisat2. We selected Hisat2 as the mapping tool for that Hisat2 can generate a database of splice junctions based on the gene model annotation file and thus a better mapping result than other non-splice mapping tools. featureCounts (V1.5.0-p3) was used to count the reads numbers mapped to each gene. And then FPKM of each gene was calculated based on the length of the gene and reads count mapped to this gene. FPKM, expected number of Fragments Per Kilobase of transcript sequence per Millions base pairs sequenced, considers the effect of sequencing depth and gene length for the reads count at the same time, and is currently the most commonly used method for estimating gene expression levels. Differential expression analysis of two conditions/groups (two biological replicates per condition) was performed using the DESeq2 R package (V1.16.1).

Statistical Analysis

All data reported in this paper are expressed as the means ± SEMs. The data were evaluated by one-way ANOVA, Wilcox, or Mann-Whitney U tests. All statistics were analyzed by SPSS software, and all analyses were performed with GraphPad Prism 7.

Supplementary Information

Additional file 1: Table S1. Primers used in this study. **Table S2**. Key resources table.

Additional file 2: Figure S1. Effects of the LDP treatment on microniota. **Figure S2**. The relative abundances of bacteria at phylum and genus level. **Figure S3**. The long-term effects of LDP on intestinal microbiota. **Figure S4**. Changes in the metabolism of mice. **Figure S5.** Changes of the serum hormones and adipose tissue.

Declarations

Ethics approval and consent to participate

Not applicable.

Consent for publication

Not applicable.

Availability of data and materials

The RNA-seq and 16S rRNA gene sequencing data supporting this research are available on NCBI with accession number PRJNA577425. All other data that support the findings of this study are available from the corresponding author upon reasonable request.

Competing interests

The authors declare no competing interests.

Funding

The work was supported by the Research on Blueberry Functional Ingredients and the Development of New Blueberry Wine (201805410611582).

Author contributions

J.Z. and J.G. designed the study and wrote the manuscript. J.G. and X.H. performed the experiments. Y.Y. and W.H. contributed to the data analysis.

Acknowledgements

Not applicable.

References

1. Cox, L. M.; Blaser, M. J., Antibiotics in early life and obesity. *Nat Rev Endocrinol* **2015,** *11* (3), 182-90.
2. Tamburini, S.; Shen, N.; Wu, H. C.; Clemente, J. C., The microbiome in early life: implications for health outcomes. *Nat Med* **2016,** *22* (7), 713-22.
3. Cox, L. M.; Yamanishi, S.; Sohn, J.; Alekseyenko, A. V.; Leung, J. M.; Cho, I.; Kim, S. G.; Li, H.; Gao, Z.; Mahana, D.; Zarate Rodriguez, J. G.; Rogers, A. B.; Robine, N.; Loke, P.; Blaser, M. J., Altering the intestinal microbiota during a critical developmental window has lasting metabolic consequences. *Cell* **2014,** *158* (4), 705-721.
4. Cho, I.; Yamanishi, S.; Cox, L.; Methe, B. A.; Zavadil, J.; Li, K.; Gao, Z.; Mahana, D.; Raju, K.; Teitler, I.; Li, H.; Alekseyenko, A. V.; Blaser, M. J., Antibiotics in early life alter the murine colonic microbiome and adiposity. *Nature* **2012,** *488* (7413), 621-626.
5. Knoop, K. A.; Gustafsson, J. K.; McDonald, K. G.; Kulkarni, D. H.; Coughlin, P. E.; McCrate, S.; Kim, D.; Hsieh, C.-S.; Hogan, S. P.; Elson, C. O., Microbial antigen encounter during a preweaning interval is critical for tolerance to gut bacteria. *Science immunology* **2017,** *2* (18), eaao1314.
6. Rogier, E. W.; Frantz, A. L.; Bruno, M. E.; Wedlund, L.; Cohen, D. A.; Stromberg, A. J.; Kaetzel, C. S., Secretory antibodies in breast milk promote long-term intestinal homeostasis by regulating the gut microbiota and host gene expression. *Proceedings of the National Academy of Sciences* **2014,** *111* (8), 3074-3079.

7. Mirpuri, J.; Raetz, M.; Sturge, C. R.; Wilhelm, C. L.; Benson, A.; Savani, R. C.; Hooper, L. V.; Yarovinsky, F., Proteobacteria-specific IgA regulates maturation of the intestinal microbiota. *Gut Microbes* **2014,** *5* (1), 28-39.
8. Saari, A.; Virta, L. J.; Sankilampi, U.; Dunkel, L.; Saxen, H., Antibiotic exposure in infancy and risk of being overweight in the first 24 months of life. *Pediatrics* **2015,** *135* (4), 617-626.
9. Risnes, K. R.; Belanger, K.; Murk, W.; Bracken, M. B., Antibiotic exposure by 6 months and asthma and allergy at 6 years: findings in a cohort of 1,401 US children. *American journal of epidemiology* **2011,** *173* (3), 310-318.
10. Sun, Q.; Dyar, O. J.; Zhao, L.; Tomson, G.; Nilsson, L. E.; Grape, M.; Song, Y.; Yan, L.; Lundborg, C. S., Overuse of antibiotics for the common cold–attitudes and behaviors among doctors in rural areas of Shandong Province, China. *BMC Pharmacology and Toxicology* **2015,** *16* (1), 6.
11. Ying, G.-G.; He, L.-Y.; Ying, A. J.; Zhang, Q.-Q.; Liu, Y.-S.; Zhao, J.-L., China must reduce its antibiotic use. *Environmental Science & Technology* **2017**, 1072-1073.
12. Brüssow, H., Adjuncts and alternatives in the time of antibiotic resistance and in-feed antibiotic bans. *Microbial biotechnology* **2017,** *10* (4), 674.
13. Wu, Z., Antibiotic use and antibiotic resistance in food-producing animals in China. **2019**.
14. Wang, H.; Ren, L.; Yu, X.; Hu, J.; Chen, Y.; He, G.; Jiang, Q., Antibiotic residues in meat, milk and aquatic products in Shanghai and human exposure assessment. *Food control* **2017,** *80*, 217-225.
15. Delatour, T.; Racault, L.; Bessaire, T.; Desmarchelier, A., Screening of veterinary drug residues in food by LC-MS/MS. Background and challenges. *Food Additives & Contaminants: Part A* **2018,** *35* (4), 633-646.
16. Schulfer, A. F.; Schluter, J.; Zhang, Y.; Brown, Q.; Pathmasiri, W.; McRitchie, S.; Sumner, S.; Li, H.; Xavier, J. B.; Blaser, M. J., The impact of early-life sub-therapeutic antibiotic treatment (STAT) on excessive weight is robust despite transfer of intestinal microbes. *The ISME journal* **2019,** *13* (5), 1280-1292.
17. Zhang, X.-S.; Li, J.; Krautkramer, K. A.; Badri, M.; Battaglia, T.; Borbet, T. C.; Koh, H.; Ng, S.; Sibley, R. A.; Li, Y., Antibiotic-induced acceleration of type 1 diabetes alters maturation of innate intestinal immunity. *Elife* **2018,** *7*, e37816.
18. Ruiz, V. E.; Battaglia, T.; Kurtz, Z. D.; Bijnens, L.; Ou, A.; Engstrand, I.; Zheng, X.; Iizumi, T.; Mullins, B. J.; Müller, C. L., A single early-in-life macrolide course has lasting effects on murine microbial network topology and immunity. *Nature communications* **2017,** *8* (1), 1-14.
19. Guo, J.; Han, X.; Huang, W.; You, Y.; Jicheng, Z., Interaction between IgA and gut microbiota and its role in controlling metabolic syndrome. *Obesity Reviews* **2020**.
20. Guo, J. L.; Han, X.; Zhan, J. C.; You, Y. L.; Huang, W. D., Vanillin Alleviates High Fat Diet-Induced Obesity and Improves the Gut Microbiota Composition. *Frontiers In Microbiology* **2018,** *9:2733.*
21. Guo, J.; Han, X.; Huang, W.; You, Y.; Jicheng, Z., Interaction between IgA and gut microbiota and its role in controlling metabolic syndrome. *Obesity Reviews* **2021,** *22* (4), e13155.

22. Penicillin V for bacterial infections. https://www.medicinesforchildren.org.uk/penicillin-v-bacterial-infections.
23. Al Nabhani, Z.; Dulauroy, S.; Marques, R.; Cousu, C.; Al Bounny, S.; Dejardin, F.; Sparwasser, T.; Berard, M.; Cerf-Bensussan, N.; Eberl, G., A Weaning Reaction to Microbiota Is Required for Resistance to Immunopathologies in the Adult. *Immunity* **2019,** *50* (5), 1276-1288 e5.
24. Ramanan, D.; Sefik, E.; Galván-Peña, S.; Wu, M.; Yang, L.; Yang, Z.; Kostic, A.; Golovkina, T. V.; Kasper, D. L.; Mathis, D., An immunologic mode of multigenerational transmission governs a gut Treg setpoint. *Cell* **2020**.
25. Macpherson, A. J.; Gatto, D.; Sainsbury, E.; Harriman, G. R.; Hengartner, H.; Zinkernagel, R. M., A primitive T cell-independent mechanism of intestinal mucosal IgA responses to commensal bacteria. *Science* **2000,** *288* (5474), 2222-2226.
26. Yang, C.; Mogno, I.; Contijoch, E. J.; Borgerding, J. N.; Aggarwala, V.; Li, Z.; Siu, S.; Grasset, E. K.; Helmus, D. S.; Dubinsky, M. C., Fecal IgA Levels Are Determined by Strain-Level Differences in Bacteroides ovatus and Are Modifiable by Gut Microbiota Manipulation. *Cell host & microbe* **2020**.
27. Mesin, L.; Di Niro, R.; Thompson, K. M.; Lundin, K. E.; Sollid, L. M., Long-lived plasma cells from human small intestine biopsies secrete immunoglobulins for many weeks in vitro. *The Journal of Immunology* **2011,** *187* (6), 2867-2874.
28. Bunker, J. J.; Flynn, T. M.; Koval, J. C.; Shaw, D. G.; Meisel, M.; McDonald, B. D.; Ishizuka, I. E.; Dent, A. L.; Wilson, P. C.; Jabri, B., Innate and adaptive humoral responses coat distinct commensal bacteria with immunoglobulin A. *Immunity* **2015,** *43* (3), 541-553.
29. Chassaing, B.; Koren, O.; Goodrich, J. K.; Poole, A. C.; Srinivasan, S.; Ley, R. E.; Gewirtz, A. T., Dietary emulsifiers impact the mouse gut microbiota promoting colitis and metabolic syndrome. *Nature* **2015,** *519* (7541), 92-6.
30. Ghorpade, D. S.; Ozcan, L.; Zheng, Z.; Nicoloro, S. M.; Shen, Y.; Chen, E.; Blüher, M.; Czech, M. P.; Tabas, I., Hepatocyte-secreted DPP4 in obesity promotes adipose inflammation and insulin resistance. *Nature* **2018,** *555* (7698), 673.
31. Batterham, R. L.; Heffron, H.; Kapoor, S.; Chivers, J. E.; Chandarana, K.; Herzog, H.; Le Roux, C. W.; Thomas, E. L.; Bell, J. D.; Withers, D. J., Critical role for peptide YY in protein-mediated satiation and body-weight regulation. *Cell metabolism* **2006,** *4* (3), 223-233.
32. Yan, J.; Herzog, J. W.; Tsang, K.; Brennan, C. A.; Bower, M. A.; Garrett, W. S.; Sartor, B. R.; Aliprantis, A. O.; Charles, J. F., Gut microbiota induce IGF-1 and promote bone formation and growth. *Proceedings of the National Academy of Sciences* **2016,** *113* (47), E7554-E7563.
33. Renehan, A. G.; Frystyk, J.; Flyvbjerg, A., Obesity and cancer risk: the role of the insulin–IGF axis. *Trends in Endocrinology & Metabolism* **2006,** *17* (8), 328-336.
34. Suez, J.; Zmora, N.; Zilberman-Schapira, G.; Mor, U.; Dori-Bachash, M.; Bashiardes, S.; Zur, M.; Regev-Lehavi, D.; Ben-Zeev Brik, R.; Federici, S.; Horn, M.; Cohen, Y.; Moor, A. E.; Zeevi, D.; Korem, T.; Kotler, E.; Harmelin, A.; Itzkovitz, S.; Maharshak, N.; Shibolet, O.; Pevsner-Fischer, M.; Shapiro, H.; Sharon, I.;

Halpern, Z.; Segal, E.; Elinav, E., Post-Antibiotic Gut Mucosal Microbiome Reconstitution Is Impaired by Probiotics and Improved by Autologous FMT. *Cell* **2018,** *174* (6), 1406-1423 e16.

35. Bunker, J. J.; Bendelac, A., IgA Responses to Microbiota. *Immunity* **2018,** *49* (2), 211-224.
36. Li, H.; Limenitakis, J. P.; Greiff, V.; Yilmaz, B.; Schären, O.; Urbaniak, C.; Zünd, M.; Lawson, M. A.; Young, I. D.; Rupp, S., Mucosal or systemic microbiota exposures shape the B cell repertoire. *Nature* **2020,** *584* (7820), 274-278.
37. Pabst, O., New concepts in the generation and functions of IgA. *Nat Rev Immunol* **2012,** *12* (12), 821-32.
38. Hapfelmeier, S.; Lawson, M. A.; Slack, E.; Kirundi, J. K.; Stoel, M.; Heikenwalder, M.; Cahenzli, J.; Velykoredko, Y.; Balmer, M. L.; Endt, K., Reversible microbial colonization of germ-free mice reveals the dynamics of IgA immune responses. *Science* **2010,** *328* (5986), 1705-1709.
39. Luck, H.; Khan, S.; Kim, J. H.; Copeland, J. K.; Revelo, X. S.; Tsai, S.; Chakraborty, M.; Cheng, K.; Chan, Y. T.; Nøhr, M. K., Gut-associated IgA+ immune cells regulate obesity-related insulin resistance. *Nature communications* **2019,** *10* (1), 1-17.
40. Tran, H. Q.; Ley, R. E.; Gewirtz, A. T.; Chassaing, B., Flagellin-elicited adaptive immunity suppresses flagellated microbiota and vaccinates against chronic inflammatory diseases. *Nat Commun* **2019,** *10* (1), 5650.
41. Jiang, T. T.; Shao, T. Y.; Ang, W. X. G.; Kinder, J. M.; Turner, L. H.; Pham, G.; Whitt, J.; Alenghat, T.; Way, S. S., Commensal Fungi Recapitulate the Protective Benefits of Intestinal Bacteria. *Cell host & microbe* **2017,** *22* (6), 809-816 e4.
42. Iliev, I. D.; Funari, V. A.; Taylor, K. D.; Nguyen, Q.; Reyes, C. N.; Strom, S. P.; Brown, J.; Becker, C. A.; Fleshner, P. R.; Dubinsky, M., Interactions between commensal fungi and the C-type lectin receptor Dectin-1 influence colitis. *Science* **2012,** *336* (6086), 1314-1317.
43. Daims, H.; Brühl, A.; Amann, R.; Schleifer, K.-H.; Wagner, M., The domain-specific probe EUB338 is insufficient for the detection of all Bacteria: development and evaluation of a more comprehensive probe set. *Systematic and applied microbiology* **1999,** *22* (3), 434-444.
44. Haas, B. J.; Gevers, D.; Earl, A. M.; Feldgarden, M.; Ward, D. V.; Giannoukos, G.; Ciulla, D.; Tabbaa, D.; Highlander, S. K.; Sodergren, E., Chimeric 16S rRNA sequence formation and detection in Sanger and 454-pyrosequenced PCR amplicons. *Genome research* **2011,** *21* (3), 494-504.

Figures

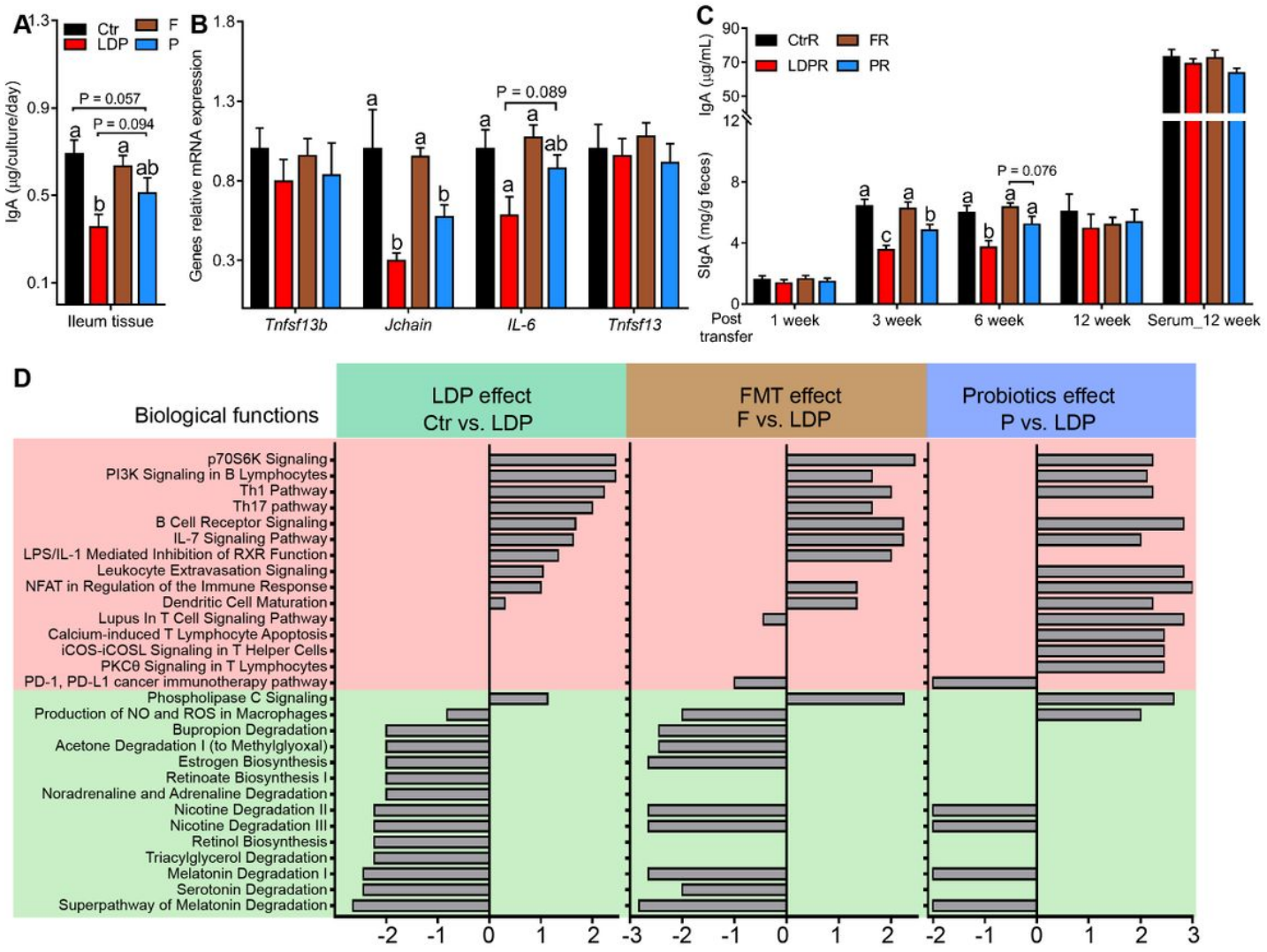

Figure 1

Microbiota disturbed by LDP-treatment. (A) Study design, details are specified in the main text. (B and C) The principal coordinate analysis (PCoA) based on the weighted UniFrac distance indicated the differences in the bacterial composition of ileal mucosal (B) and colonic luminal (C) samples among the four groups. Significance was determined using the Adonis test. (D) Discrepant bacterial species of the ileal mucosal samples between the LDP and the Ctr mice identified by LEfSe analysis. (E and F) The relative abundance of Candidatus Arthromitus (E) and Lactobacillus (F) from the different intestinal regions, as determined by 16S rRNA gene sequencing. Different letters indicate a significant difference between the columns, $p < 0.05$. Differences were determined by LSD posthoc tests of one-way ANOVA as compared to Dunnett's (T3) test. For all figures, n = 5 for the Ctr mice, n = 7 for the LDP mice, and n = 6 for the F and P mice.

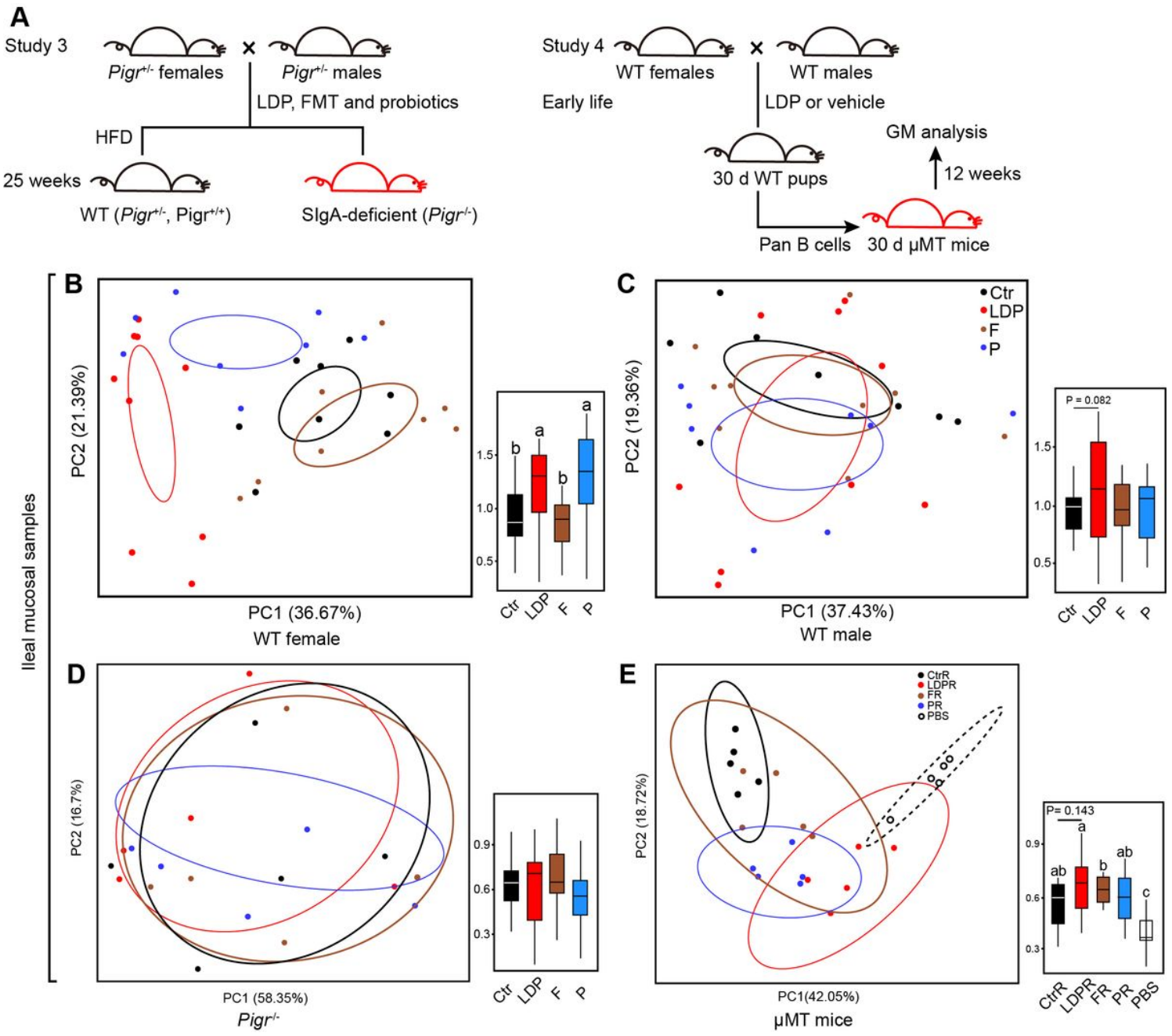

Figure 2

LDP persistently dampened IgA responses. (A) Study design of mouse Study 2, details was specified in the main text. (B) Changes in fecal SIgA levels. *P < 0.05 and **P < 0.01 as compared to LDP mice; #P < 0.05, ##P < 0.01, and ###P < 0.001 as compared to HDP mice. Different colors indicate different groups: Black for Ctr, brown for F, and blue for P group. N = 10–13 for each group. Differences were determined by Mann-Whitney U test. (C) Caecal SIgA levels in 30-d-old and 25-week-old mice. (D–G) Frequency and absolute number of IgA-producing B cells (IgA+ B220+) and plasma cells (IgA+ B220-) within the distal small intestine lamina propira (D and E) and Peyer's patches (F and G) in 30-d-old (D and F) and 25-week-old (E and G) female mice. For C to G, n = 5 for all 30 day mice, n = 5–8 for 25 week mice. Different letters indicate a significant difference between columns, p < 0.05; differences were determined by LSD post hoc test or one-way ANOVA as compared to Dunnett's test (T3).

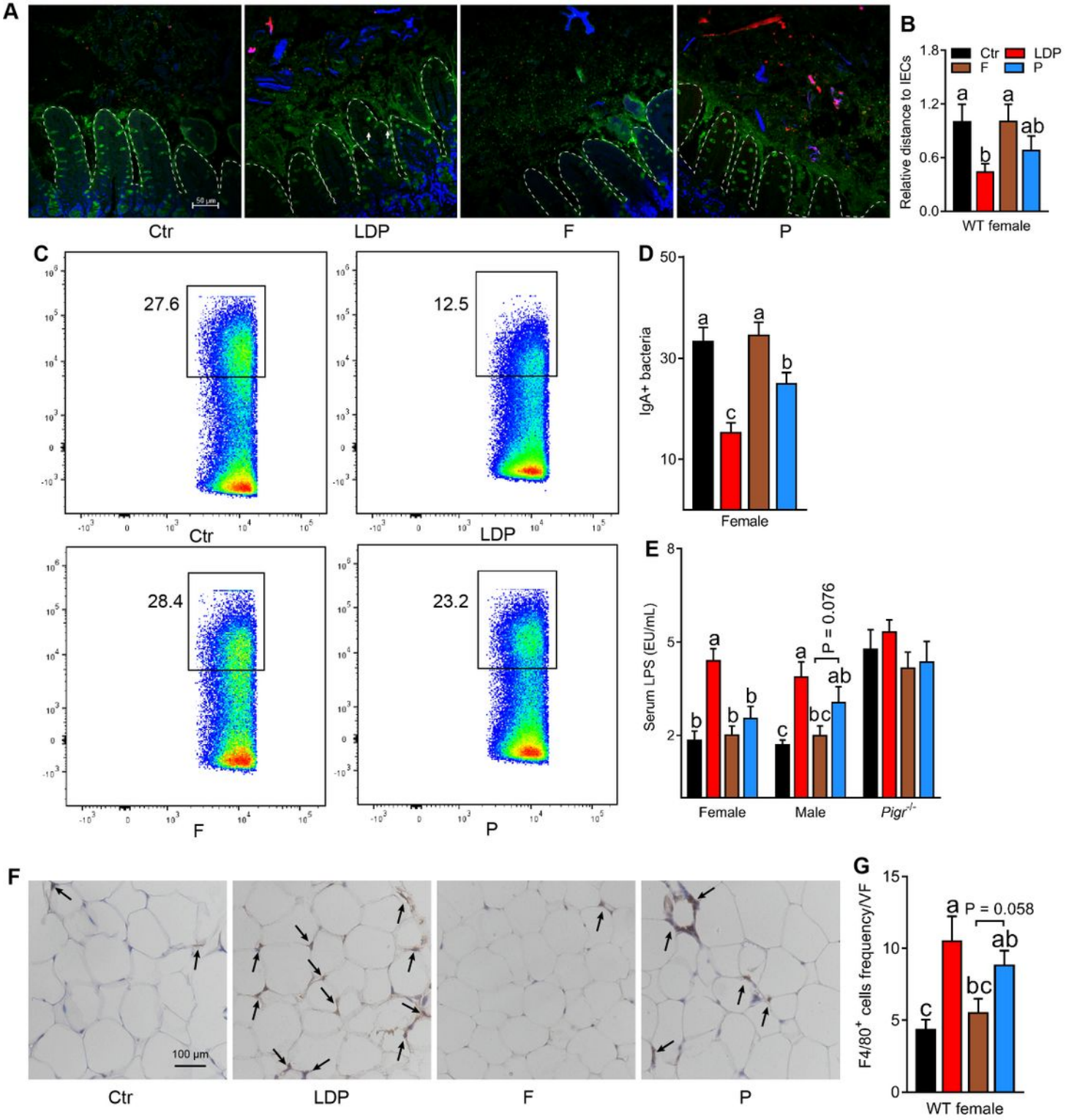

Figure 3

LDP-induced inhibition of IgA was GM- and early life-dependent. (A and B) IgA production (A) and relative gene expression (B) in the mouse ileum during in vitro cultivation with fecal microbiota derived from the Ctr, LDP, F, and P mice, n = 4. (C) The fecal SIgA levels of the conventionalized GF mice transferred fecal microbiota from 30-d-old Ctr, LDP, F, and P mice, where n = 8 for all treatments. (J) Predicted canonical pathways determined by Ingenuity Pathway Analysis of the RNA-sequencing of ileal gene expression.

Different letters indicate a significant difference between columns, p < 0.05; differences were determined by LSD post hoc test or one-way ANOVA as compared to Dunnett's test (T3).

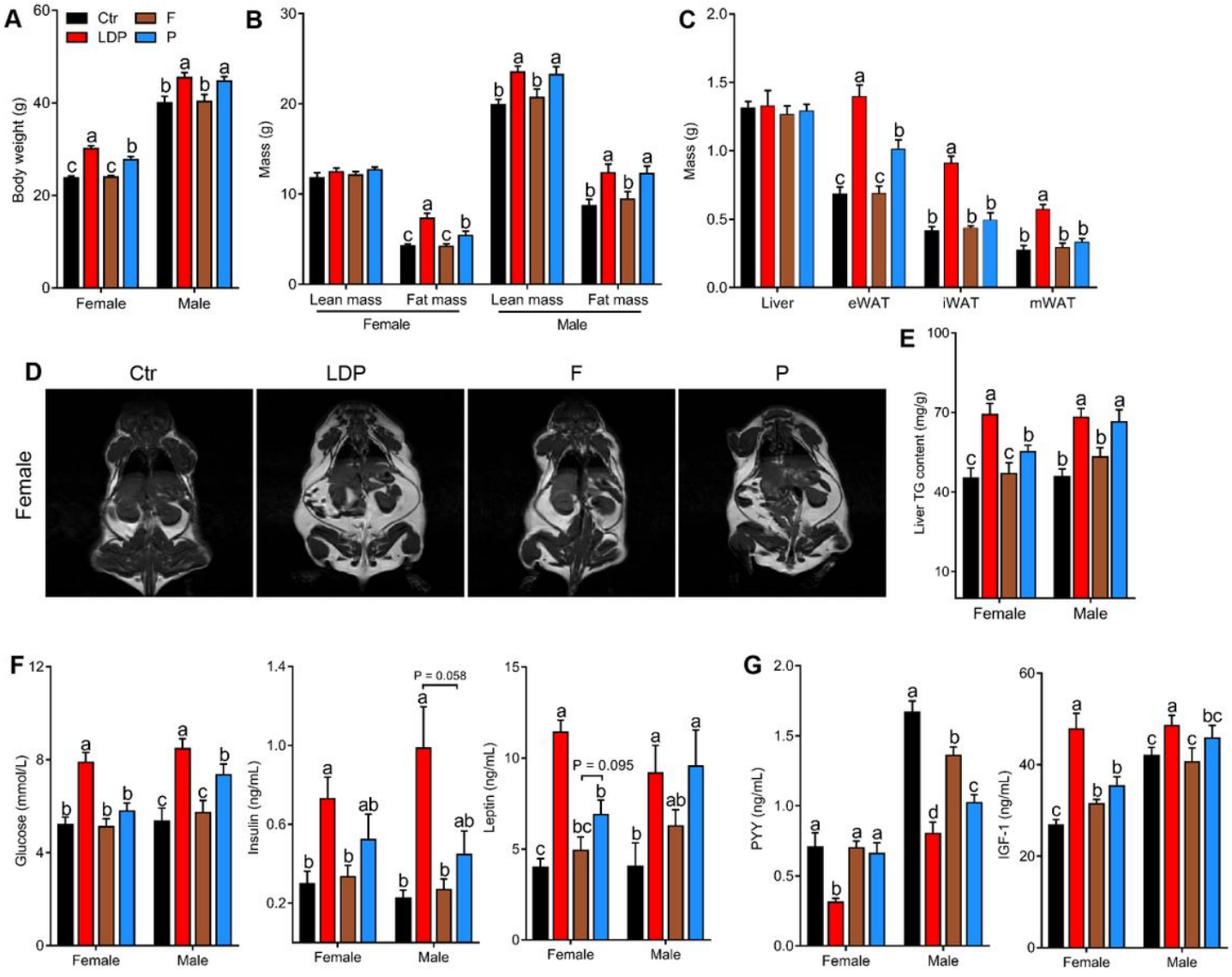

Figure 4

LDP persistently disturbed ileal microbiota in a SIgA-dependent manner. (A) Study design, details were specified in the main text. (B–E) PCoA analysis based on weighted UniFrac distance showed the differences in ileal mucosal bacterial composition from 25-week-old WT females (B) and males (C) and Pigr-/- females (D) and 15-week-old μMT (B cell-deficient) females (E). N = 8–9 for WT mice and n = 5 for Pigr-/- and μMT mice. Different letters indicate a significant difference between columns, P < 0.05, as determined by Adonis test.

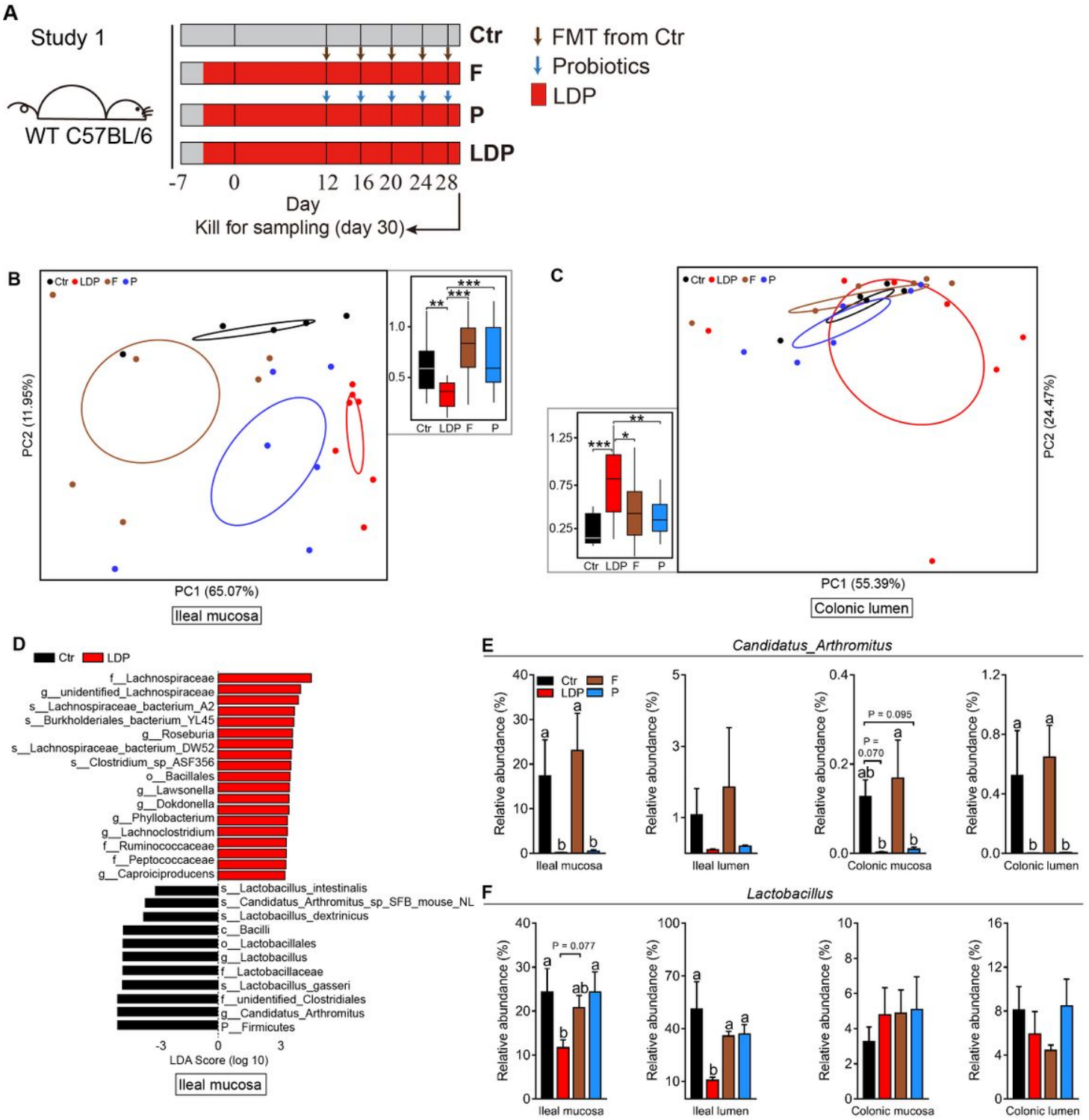

Figure 5

LDP increased bacterial encroachment and adipose inflammation in a SIgA-dependent manner in mice from Study 3. (A) Representative confocal microscopy analysis of ileal bacterial localization in WT females: MUC 2, green; bacteria, red; and DNA, blue; white arrow, invasive bacteria. n = 3. Distances of bacteria that translocate into the villi are calculated as zero. (B) Relative distance of the closest bacteria to intestinal epithelial cells (IECs) over five high-powered fields per WT (B). (C and D) Proportion of ileal IgA+ bacteria in WT females; n = 8–9. (E) Serum lipopolysaccharides concentration; n = 8–9. (F and G)

Representative immunohistochemical analysis targeting F4/80 in visceral adipose tissue of WT females; n = 3. Black arrow, F4/80+ cells. Different letters indicate a significant difference between columns, $p < 0.05$; differences were determined by LSD post hoc test or one-way ANOVA as compared to Dunnett's test (T3).

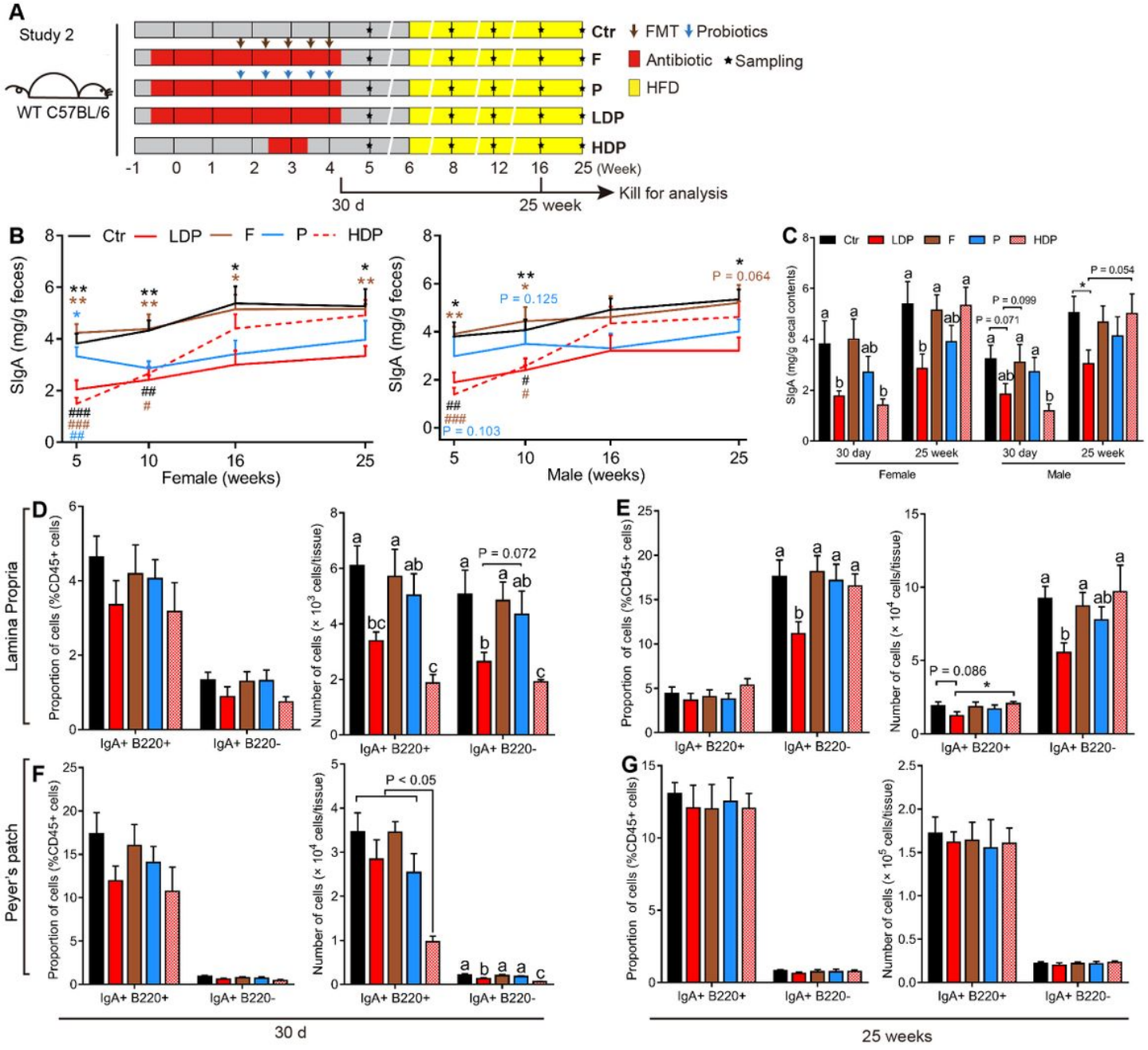

Figure 6

LDP enhanced diet-induced MetS. (A–G) Metabolic parameters of 25-week-old WT mice in Study 3. (A–C) Body (A), lean/fat (B), and tissue (C) masses. (D) Representative MRI images of the 25-week-old females; the white areas represent lipids, n = 3 for each group. (E) Hepatic triglyceride (TG) contents. (F) Serum levels of glucose (left), insulin (middle), and leptin (right). (F) Serum levels of peptide YY (PYY, left) and Insulin-like growth factor 1 (IGF-1, right). N = 8–9 for all figures except D. Different letters indicate a

significant difference between columns, $p < 0.05$; differences were determined by LSD post hoc test or one-way ANOVA as compared to Dunnett's test (T3).

Supplementary Files

This is a list of supplementary files associated with this preprint. Click to download.

- Additionalfile1.docx
- Additionalfile2.docx